

From Solution to Langmuir–Blodgett Films: Spectroscopic Study of a Zwitterionic Dye

Francesca Terenziani, Anna Painelli,* and Alberto Girlando

Dipartimento di Chimica GIAF and INSTM UdR–Parma, Università di Parma, viale delle Scienze 17/a, 43100 Parma, Italy

Robert M. Metzger

Laboratory for Molecular Electronics, Department of Chemistry, University of Alabama, Box 870336, Tuscaloosa, Alabama 35487-0336

Received: May 13, 2004; In Final Form: May 19, 2004

We present a thorough spectroscopic study of γ -(*n*-hexadecyl)quinolinium tricyanoquinodimethanide, C₁₆H₃₃Q-3CNQ, a very well-known zwitterionic donor- π -acceptor chromophore, that behaves as a molecular rectifier. Absorption and Raman spectra are collected from solution and solid samples, as well as from Langmuir–Blodgett (LB) monolayer and multilayers. Whereas Raman spectra confirm the zwitterionic nature of the molecule in all phases, the absorption spectra show a complex evolution with the molecular environment. The impressive inverse solvatochromic behavior (hypsochromism) shown by C₁₆H₃₃Q-3CNQ is analyzed, based on the Mulliken–Holstein model that was previously used to describe spectral properties of normal solvatochromic (bathochromic) dyes. The same model is extended here to describe the molecular units in the LB monolayer. Intermolecular interactions in the film are introduced as classical electrostatic forces. The molecular parameters entering the model are extracted from the analysis of absorption and emission spectra in solution in a bottom-up modeling that allows the transfer of information among the different phases. The polarity of the ground state is estimated as $\rho \approx 0.89, 0.90$, and 0.93 in CHCl₃, CH₂Cl₂, and CH₃CN, respectively. The ground and first excited-state electric dipole moment at infinite dilution in CH₂Cl₂ are estimated as 36 and 4 D, respectively, in good agreement with previous estimates. The large blue-shift of the absorption band in the LB film with respect to solution is ascribed to the increased polarity of the environment, rather than to excitonic effects.

1. Introduction

D- π -A chromophores are an interesting class of molecules, where an electron-donor (D) and an electron-acceptor (A) group are linked by a π -conjugated bridge.^{1–3} These molecules have been dubbed “pp chromophores”, pp standing for push–pull. Here, we prefer to reinterpret the pp acronym to mean polar and polarizable, making direct reference to their distinguishing physical properties.⁴ The low-energy physics of pp chromophores is governed by the resonance between a neutral, DA, and a charge-separated (zwitterionic), D⁺A[−], state.^{5–7} An intense absorption between these two states, associated with intramolecular charge transfer (CT) or intervalence transfer (IVT), is observed in the visible region of the spectrum. The transition exhibits an important dependence on the polarity of the environment, so that pp chromophores are widely used as solvation and polarity probes.⁸ This same transition is responsible for the large emission quantum yields of many chromophores,^{4,8} and for their large NLO responses. Thanks to the lack of inversion symmetry, pp chromophores are the molecules of choice for second-order NLO applications.^{1–3} Indeed γ -(*n*-hexadecyl)quinolinium tricyanoquinodimethanide (C₁₆H₃₃Q-3CNQ) in Figure 1 was originally synthesized for NLO purposes, and when deposited as a Z-type (acentric) Langmuir–Blodgett (LB) film, it exhibited large second-order NLO responses.⁹

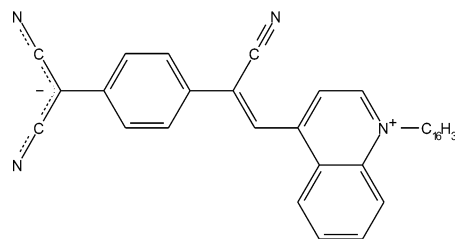


Figure 1. Molecular structure of C₁₆H₃₃Q-3CNQ.

This same molecule proved even more interesting in the different, but actually not fully unrelated, field of molecular electronics: LB films of C₁₆H₃₃Q-3CNQ offered the first demonstration of molecular electrical rectification.^{10,11} On a more fundamental vein, pp chromophores are interesting model systems for investigating charge and electron-transfer processes¹² and the associated environmental effects.¹³ The very basic definition of functional (or intelligent) materials implies materials that behave in a qualitatively different way depending on the applied inputs: functional behavior is just a manifestation of nonlinear behavior. It is then not accidental that interesting molecular materials for application in photonics, optoelectronics, and molecular electronics are most often made up of large π -conjugated molecules, whose nonlinearity is very well-known.^{3,14} Supramolecular interactions in molecular materials made up of largely polarizable molecules are particularly important: collective and cooperative effects were predicted

* Address correspondence to this author.

more than 40 years ago to largely affect the material behavior.¹⁵ In molecular materials based on pp chromophores the polar molecular environment affects in a highly nontrivial way the polarizable molecular units in a feedback mechanism that leads to interesting and new physics.^{16,17} Studying the same molecule in solution as well as in condensed phases, including specially engineered phases like LB or self-assembled films, offers a unique opportunity to investigate the role of supramolecular interactions in molecular materials. This is one of the fundamental problems in modern material chemistry, with particularly important implications in the specific field of functional molecular materials.

C₁₆H₃₃Q-3CNQ is an interesting chromophore in several respects: its inverse solvatochromic (hypsochromic) behavior puts it among the few zwitterionic dyes with no net molecular charge.¹⁸ Good LB films form on different substrates and the relevant optical spectra distinctively differ from solution spectra.^{18–20} In this paper we present a step-by-step approach to the physics of materials based on C₁₆H₃₃Q-3CNQ. A detailed analysis of absorption and emission spectra of C₁₆H₃₃Q-3CNQ in different solvents is presented in Section 3. The Mulliken–Holstein model that was recently proposed to describe solvatochromic behavior of pp chromophores with normal solvatochromism (bathochromism)⁴ is applied here for the first time to a hypsochromic dye. The model nicely describes the evolution of the absorption and emission frequencies, intensities, and band-shapes with solvent polarity, based on a few molecular parameters that are kept constant. Tuning a single parameter is enough to account for the complex effects of the solvent polarity on absorption and emission spectra. This first step in our work offers new and important clues to the current understanding of polar solvation, but also sets the stage for modeling the behavior of C₁₆H₃₃Q-3CNQ in different environments. The model defined in Section 3 for the solvated molecule is in fact adopted in Section 4 to describe electronic spectra of LB films of C₁₆H₃₃Q-3CNQ. Supramolecular effects enter the model as classical electrostatic interactions that can be modeled for any specific supramolecular arrangement.^{16,17} The direct solution of the relevant many-body Hamiltonian leads us to a good understanding of supramolecular effects on the material properties and specifically on its spectral behavior. The relevance of these results in a wider context is briefly addressed in Section 5.

2. Experimental Section

C₁₆H₃₃Q-3CNQ was synthesized as described in ref 10. LB films of C₁₆H₃₃Q-3CNQ were deposited on different substrates (either quartz or gold), according to the procedure described in ref 10. C₁₆H₃₃Q-3CNQ does not dissolve at all in apolar solvents, and is poorly soluble in most organic solvents. Solutions in spectrophotometric grade CHCl₃, CH₂Cl₂, and CH₃CN (from Aldrich) were obtained up to concentrations of $\sim 10^{-5}$ M. Absorption spectra in solution were collected on a Bruker IFS66 FT spectrometer equipped with a quartz beam-splitter, a Tungsten source, and a Si detector. The spectrometer has a good response in the spectral region of interest, so that reliable absolute intensities have been measured. We devoted particular care to rule out aggregation phenomena. Specifically, we verified the Lambert–Beer law in all solvents, measuring spectra in solutions whose concentration was varied from $\sim 10^{-5}$ to $\sim 10^{-6}$ M. The absorption spectra of C₁₆H₃₃Q-3CNQ powders dispersed in Nujol and of LB films on quartz were collected on a UV–visible Jasco Uvidec 505 spectrophotometer. Raman spectra of C₁₆H₃₃Q-3CNQ in different phases have been measured with a Renishaw System-1000 Raman microscope,

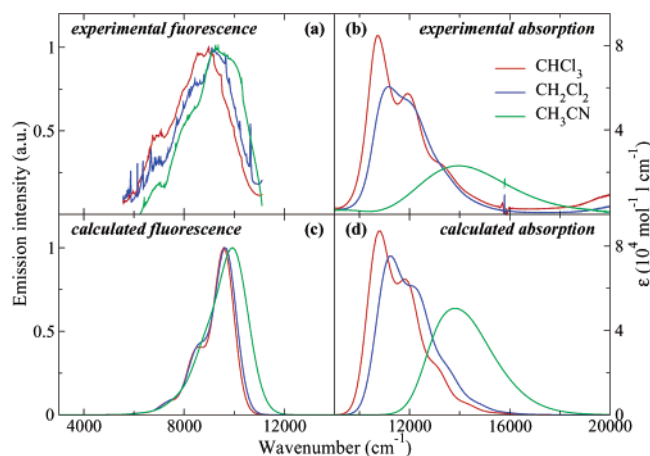


Figure 2. Upper panels: experimental (a) fluorescence and (b) absorption spectra of C₁₆H₃₃Q-3CNQ dissolved in CHCl₃ (red lines), CH₂Cl₂ (blue lines), and CH₃CN (green lines). Lower panels: calculated (c) fluorescence and (d) absorption spectra for the parameter listed in Table 1.

with a spectral resolution of ~ 2 cm⁻¹. All spectra were obtained upon excitation with the line at 568 nm of a Krypton ion laser. Fluorescence spectra are taken from ref 18. They were collected with a SPEX fluoromax-2 spectrometer, equipped with a Ge-diode detector, for good response in the near-infrared region. By calibration against the singlet oxygen emission band at 1270 nm, the uncertainty in the location of observed maxima is estimated as not larger than ± 5 nm.

3. Extracting Molecular Parameters from Solution Spectra

The absorption and fluorescence spectra of C₁₆H₃₃Q-3CNQ in CHCl₃, CH₂Cl₂, and CH₃CN are reported in the top panels of Figure 2. Absorption spectra in Figure 2b illustrate the already known¹⁸ large inverse solvatochromism (hypsochromism) of C₁₆H₃₃Q-3CNQ: the absorption maximum shifts to the blue by ~ 3200 cm⁻¹ as the polarity of the solvent increases from CHCl₃ to CH₃CN. Inverse solvatochromism is typical of zwitterionic dyes, i.e., of dyes whose ground state (gs) is dominated by the charge-separated (D⁺A⁻) state, the electronic excitation yielding back-CT toward an almost neutral (DA) state.⁸ The molecular dipole moment decreases upon photoexcitation, and in polar solvents the gs is more strongly stabilized than the excited state. On this basis one can easily understand why the transition energy shifts to the blue with the solvent polarity. The zwitterionic nature of C₁₆H₃₃Q-3CNQ is confirmed by the large dipole moment, $\mu_G = 43 \pm 8$ D, measured in CH₂Cl₂.¹⁰ The above sketched description of the inverse solvatochromism captures the basic physics of the process, but cannot address the subtle evolution of optical spectra with the solvent polarity, as shown in Figure 2. In particular, emission frequencies are barely affected by the solvent polarity (cf. Figure 2a), whereas the shifts in the absorption spectra are very large. Moreover, the absorption band shapes exhibit a pronounced evolution with the solvent polarity. Finally, absorption and emission band shapes are nonspecular, a feature particularly evident for strongly polar solvents such as CH₃CN.

In recent years we have proposed a model to describe the spectroscopic properties of solvated pp chromophores.^{4,21,22} The model quite successfully described the solvent dependence of electronic and vibrational spectra of pp chromophores with normal solvatochromic behavior,^{4,23} i.e., of chromophores whose gs is dominated by the neutral (DA) resonant structure. It also

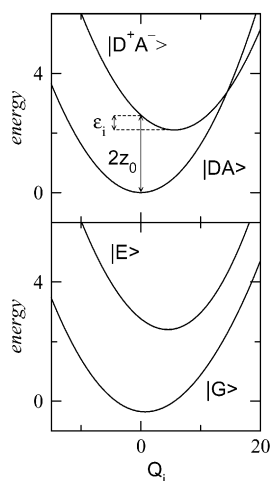


Figure 3. The potential energy surfaces for a single coupled mode relevant to the two basis states ($\sqrt{2}t = 0$, top panel) and to the adiabatic eigenstates (bottom panel).

proved successful to describe time-resolved spectra,^{24,25} showing that the proposed approach to polar solvation catches the basic physics of this complex and fascinating phenomenon. We now apply the same model to describe the spectroscopic behavior of C₁₆H₃₃Q-3CNQ, an inverse solvatochromic dye. The low-energy physics of pp chromophores is governed by the charge transfer (CT) between D and A sites: we therefore describe their electronic structure based on a very well-known two-state model, originally proposed by Mulliken²⁶ to describe CT complexes in solution and later applied to pp chromophores by several authors.^{5,6,27–29} The two basis states correspond to the two limiting resonating forms of pp chromophores, $|DA\rangle$ and $|D^+A^-\rangle$. These two states are separated by an energy gap, $2z_0$, and are mixed by a matrix element $-\sqrt{2}t$ as to originate fractional ionicity on D and A sites. Specifically, we define ρ as the weight of $|D^+A^-\rangle$ in the gs, leading to fractional ionicity in the gs: $|D^+ \rho A^- \rho\rangle$. The excited state, orthogonal to the gs, has partial ionicity $1 - \rho$. The ionicity, ρ , is a unique function of the z_0/t ratio, and fully defines the electronic ground and excited states.^{6,7} Following Mulliken,²⁶ we recognize that among the matrix elements of the dipole moment operator on the basis states, $\mu_0 = \langle D^+A^- | \hat{\mu} | D^+A^- \rangle$ is largely dominant. By neglecting all other contributions, the ground- and excited-state dipole moments are simply defined as $\mu_0\rho$ and $\mu_0(1 - \rho)$, respectively, whereas the transition dipole moment is $\mu_0\sqrt{\rho(1-\rho)}$.⁶

Vibrational degrees of freedom enter the model, since the two resonating structures have, in general, different geometry: to account for that we introduce Holstein coupling to a few vibrational coordinates.^{6,7} Specifically, we assign to the two basis states two harmonic potential energy surfaces (PES), with the same curvature, but with displaced minima along relevant coordinates. Each coupled coordinate, Q_i , is then defined by the harmonic reference frequency, ω_i , and by the small polaron binding energy, ϵ_i , measuring the relaxation energy of the $|D^+A^-\rangle$ PES along each vibrational coordinate, as sketched in Figure 3.

Within the adiabatic approximation, the electronic problem is diagonalized at fixed nuclei. In the presence of Holstein coupling, the energy gap between the two basis states becomes Q dependent and, as a consequence, all electronic properties (including ρ) vary with Q . The ground- and excited-state PES can then be obtained from the diagonalization of the electronic Hamiltonian.²¹ The resulting adiabatic PES are clearly anharmonic, as seen in the bottom panel of Figure 3.

The solvent is described as a continuum dielectric medium, and the interaction with a polar solute is modeled in terms of a reaction field. As has been discussed in detail in ref 7, the electronic contribution to the reaction field enters the model via a renormalization of electronic parameters. Since this contribution is governed by the solvent refractive index, we assume it to be independent of the solvent. The molecular electronic parameters then apply to the solvated molecule, and in general differ appreciably from those relevant to the gas-phase molecule. The polar or reorientational contribution to the reaction field enters the Hamiltonian via the definition of an effective solvation coordinate Q_0 , coupled à la Holstein with the electronic degrees of freedom.^{4,7} The strength of the relevant coupling, ϵ_{or} , measures the solvent relaxation energy accompanying the process $|DA\rangle \rightarrow |D^+A^-\rangle$, and increases with the solvent polarity. The main difference between solvation and vibrational coordinates is in the very low frequency associated with the solvation mode and in its intrinsically over-damped nature. The solvation coordinate is therefore treated as a classical coordinate, so that, at finite temperature, a Boltzmann distribution on different solvent configurations, as described by Q_0 , is responsible for the inhomogeneous broadening in the steady-state spectra.²²

We emphasize that, provided a microscopic model for the solute–solvent interaction is defined, explicit expressions can be obtained relating ϵ_{or} to the macroscopic properties of the solvent, like the refractive index, n , and the dielectric constant, ϵ . Just as an example, in the simplest hypothesis that the solute occupies a spherical cavity in the solvent with radius a , one gets:³⁰

$$\epsilon_{or} = \frac{\mu_0^2}{a^3} \left(\frac{\epsilon - 1}{2\epsilon + 1} - \frac{n^2 - 1}{2n^2 + 1} \right) \quad (1)$$

However, due to the approximate nature of any microscopic description of the cavity and to the somewhat arbitrary choice of the cavity radius entering the expression for ϵ_{or} , we prefer treating it as an empirical parameter, to be extracted from the experimental data. The solvent relaxation energy is then estimated from the analysis of the electronic spectra: we will check a posteriori its consistency with the microscopic model.

The above-sketched model is semiempirical, the required parameters being directly extracted from the optical spectra. Detailed information on electron–phonon coupling can in general be obtained from a systematic study of resonant Raman (RR) spectra in solvents of different polarity.^{22,23,31} However, C₁₆H₃₃Q-3CNQ is fluorescent, and RR spectra have only been obtained in strongly polar solvents such as DMSO, where the Stokes shift is wide enough to offer a spectral window for Raman measurements. On this basis it is hard to get information on electron–vibration coupling. On the other hand, such information is strictly required only if a detailed description of vibrational spectra is needed: electronic spectra of pp chromophores are relatively broad, and their shape can be satisfactorily modeled by including a single effective Holstein mode whose polaron binding energy, ϵ_1 , accounts for the total strength of Holstein coupling.^{4,21,25} The relevant frequency, ω_1 , roughly corresponds to the apparent spacing between the vibronic lines in absorption spectra in CHCl₃. We do not attempt to relate this apparent vibrational frequency to the vibrational frequencies in Raman spectra: we just underline that its value, lower than the frequencies in the fingerprint region in Figure 5, suggests the presence of coupled bands at lower frequencies.

Explicit expressions for the calculation of absorption and emission spectra are given in ref 4. Calculated spectra in the

TABLE 1: Molecular Parameters for C₁₆H₃₃Q-3CNQ and the Three ϵ_{or} Values (in eV) Corresponding to the Three Solvents of Interest

z_0	$\sqrt{2}t$	ω_1	ϵ_1	ϵ_{or}		
				CHCl ₃	CH ₂ Cl ₂	CH ₃ CN
−0.25	0.47	0.14	0.17	0.20	0.23	0.40

bottom panels of Figure 2 have been obtained with the model parameters in Table 1, so as to reproduce experimental spectra. We emphasize that the molecular parameters z_0 and $\sqrt{2}t$, defining the electronic problem, and ω_1 and ϵ_1 , defining the Holstein coupling, are kept rigorously constant in all solvents. The complex spectral evolution of absorption and emission bands with the solvent polarity is thus nicely reproduced by tuning just a *single* parameter ϵ_{or} , and using exactly the same intrinsic band shape (a Gaussian with full width at half-maximum of $\sim 600 \text{ cm}^{-1}$) for *all* calculated absorption and emission spectra. The progressive smearing out of the vibronic structure observed in the absorption spectra with increasing solvent polarity, as well as the observation of different absorption and emission band shapes, are then naturally accounted for within the proposed approach, and do not require any ad hoc adjustment of the intrinsic band shape.

The comparison between experimental and calculated spectra in Figure 2 demonstrates that the proposed model, already applied to dyes with normal solvatochromism,⁴ also applies to inverse solvatochromic dyes, even if the behavior of the two classes of dyes is different in several respects. Apart from the obviously different direction of the solvatochromic shift in the two cases, we notice that the shifts are larger in absorption than in emission spectra for inverse solvatochromic dyes, whereas the opposite occurs for normal solvatochromic dyes.^{4,21} Moreover, absorption bands of zwitterionic chromophores become extremely broad in polar solvents, with effects that are much more evident than those for neutral chromophores. Polar solvation involves slow degrees of freedom, and is therefore responsible for inhomogeneous broadening in electronic and vibrational spectra.^{4,22} These effects are most evident in the complete loss of vibronic structure in the absorption spectra of C₁₆H₃₃Q-3CNQ in the strongly polar CH₃CN solvent (Figure 2, right panels). On the other hand, both hypsochromic ($\rho > 0.5$) and bathochromic ($\rho < 0.5$) chromophores become more polar with increasing solvent polarity. The effective Huang–Rhys factors go with $(1 - 2\rho)^2$, hence increase with solvent polarity for hypsochromic chromophores and decrease for bathochromic chromophores.²¹ Therefore in zwitterionic chromophores the effects due to inhomogeneous broadening in polar solvents and those related to the vibrational coupling cooperate to broaden the absorption spectra, whereas in neutral chromophores the two effects compete and the overall bandwidth is barely affected.

The observation of emission bands narrower than absorption bands is common to both neutral and zwitterionic dyes^{4,21,25} even if the more impressive effect is observed for zwitterionic chromophores in polar solvents, where absorption bands are particularly broad. Narrower emission than absorption bands are understood since, after photoexcitation, the chromophore relaxes along vibrational and solvation coordinates in the excited-state PES, and is driven toward a state where $|DA\rangle$ and $|D^+A^- \rangle$ are more mixed than in the gs.²¹ This corresponds to reduced effective Huang–Rhys factors for emission with respect to absorption.

For the parameters in Table 1, the polarity of C₁₆H₃₃Q-3CNQ is calculated to increase as $\rho \approx 0.89$, 0.90, and 0.93 in CHCl₃,

CH₂Cl₂, and CH₃CN, respectively, whereas the emission process, occurring after a complete relaxation of vibrational and solvation coordinates in the excited-state PES, leads to a nonequilibrium gs with reduced polarity, $\rho^* \approx 0.75$, 0.76, and 0.78 in the same solvents. The values of the parameters in Table 1 appear quite reasonable and consistent. The effective Holstein frequency $\omega_1 = 0.14 \text{ eV} \approx 1100 \text{ cm}^{-1}$ corresponds to what is generally found in conjugated polyenes.¹⁴ The value $\sqrt{2}t \approx 0.5 \text{ eV}$ is slightly smaller than typical estimates for pp chromophores, which range around 1 eV,^{6,7,27} but this can be understood based on the fairly large twist angle in the D–A bridge.¹¹

The proposed model nicely captures the basic features of C₁₆H₃₃Q-3CNQ solvatochromism, but the fit of experimental data is far from perfect, as it is indeed expected in view of the simplicity of the adopted model. In particular, whereas a decrease of the absorption intensity with an increase in the solvent polarity is predicted, the calculated absorption intensity in acetonitrile is too large. This discrepancy could be easily cured by accounting for an increasing twist angle in the D–A bridge with increasing molecular polarity,¹¹ which would imply decreasing $\sqrt{2}t$ with ρ . Accounting for this phenomenon would improve the quality of the fit at the expense of increasing the number of adjustable parameters: as far as the aims of the present work are concerned, we feel that the minimal model discussed above already offers a detailed enough understanding of solvent effects on electronic spectra of C₁₆H₃₃Q-3CNQ.

The dipole moment of the $|D^+A^- \rangle$ state, μ_0 , enters into the definition of the molar absorption coefficient⁴ and fixes the scale of the y-axis in Figure 2d, but does not affect the relative intensities of absorption spectra in different solvents. The comparison with the experimental oscillator strengths fixes μ_0 at $\sim 40 \text{ D}$. On the basis of μ_0 we estimate the gs dipole moment of C₁₆H₃₃Q-3CNQ, $\mu_G = \mu_0\rho \approx 36 \text{ D}$ in CH₂Cl₂, in quantitative agreement with available experimental results.¹⁰ The first excited-state dipole moment is estimated here as $\mu_E = \mu_0(1 - \rho) \approx 4 \text{ D}$. This value is close to the previous estimate of μ_E , which ranged between 3 and 9 D, namely $\mu_E = 5.53$ or 2.97 D from the ratios of the Stokes shifts between emission and absorption in two solvents, or $\mu_E = 8.7 \text{ D}$ obtained by an analysis of the solvatochromism for a molecule placed in an ellipsoidal solvent cavity of major axis 21 Å and minor axis 6.9 Å.¹⁸ On the other hand, μ_0 also enters the expression of the solvent relaxation energy in eq 1. By substituting there $\mu_0 \approx 40 \text{ D}$, corresponding to a dipole distance of about 8 Å, we get a plausible and approximately constant value ($9 \div 10 \text{ Å}$) for the radius of the solvent cavity in the three solvents. Thus ϵ_{or} scales properly with the solvent dielectric constant and refractive index.

4. Supramolecular Interactions in LB Monolayers

The absorption spectrum of the LB monolayer deposited on quartz in Figure 4 shows a narrow absorption band located at $\sim 18\,200 \text{ cm}^{-1}$ ($\sim 550 \text{ nm}$). Absorption bands for 20 and 11 LB multilayers deposited on quartz have a similar shape, but are slightly blue-shifted to ~ 563 and 570 nm , respectively.^{20,32} For the film deposited on silver the anomalies in the dispersion curve for the real and imaginary part of the dielectric constant locate the transition at $\sim 578 \text{ nm}$.²⁰ Some variation of the film structure and/or deposition process can easily explain these differences. However, since measurements were obtained with different experimental techniques and setups, we do not attach too strong a physical meaning to this frequency scattering. In any case, the absorption of C₁₆H₃₃Q-3CNQ in the LB film

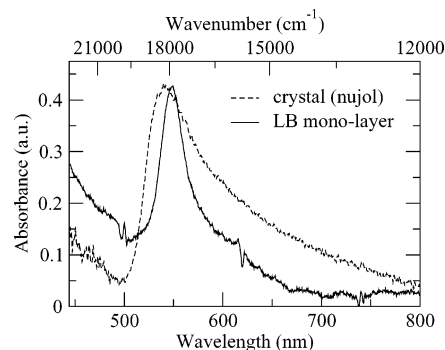


Figure 4. Visible absorption spectrum of $C_{16}H_{33}Q$ -3CNQ powders dispersed in Nujol (dashed line) and of a monolayer deposited on quartz (continuous line).

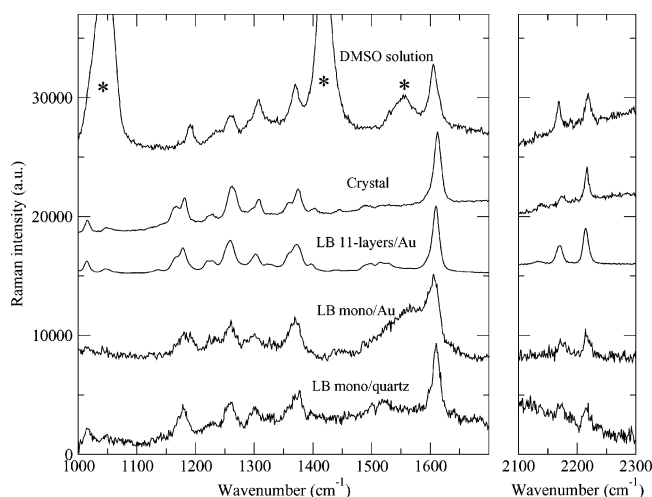


Figure 5. Raman spectra of $C_{16}H_{33}Q$ -3CNQ (from top to bottom) dissolved in DMSO, as a crystal, as an LB 11-layer deposited on Au, as an LB monolayer deposited on Au, and as an LB monolayer deposited on quartz. The star in the topmost spectrum marks solvent bands.

(550–578 nm) is strongly blue-shifted with respect to the $C_{16}H_{33}Q$ -3CNQ solutions (cf. Figure 2b), the shift amounting to ~ 4200 and 7000 cm^{-1} with respect to the spectra collected in CH_3CN and $CHCl_3$, respectively. This large shift of the absorption frequency observed for the same molecule in different environments is clear proof of the crucial role played by supramolecular interactions in pp chromophores.

The Raman spectra of $C_{16}H_{33}Q$ -3CNQ are, instead, barely affected by the environment (cf. Figure 5), suggesting that, despite the notable differences in the absorption spectra, the $C_{16}H_{33}Q$ -3CNQ molecule has a very similar structure in all phases. In particular, the position of $C\equiv N$ stretching modes, sensitive to the molecular polarity,^{33,34} is basically the same in all phases. We conclude that in LB films, either mono- or multilayers, and in the crystalline phase as well, ρ remains similar to the ~ 0.9 value estimated from the optical spectra in solution.

The blue-shift of the absorption band in the LB phases, associated with its pronounced narrowing, suggests the presence of aggregation phenomena: narrow and blue-shifted bands are usually ascribed to the presence of H-aggregates, where repulsive intermolecular interactions are responsible for an excitonic shift that increases the energy of allowed transitions.³⁸ On the other hand, based on the large solvatochromic behavior of the absorption band, the blue-shift of the absorption from solution to LB-film can also be driven by a variation of the medium polarity. In this respect, we notice that the spectrum

of the crystalline powder has an absorption band located at a frequency similar to that of the monolayer (Figure 4, dashed line). Due to the lack of good quality crystals, structural data are not available. However, in most pp crystals the polar molecular units arrange themselves in such a way as to maximize attractive intermolecular interactions, so that molecules in crystalline phases behave, in general, as in strongly polar media: the similarity with the monolayer spectra in Figure 4 then suggests that polarity effects are important. As a matter of fact the position of the absorption spectrum in LB monolayers, or more generally in supramolecular architectures of polar and polarizable molecules, is determined by a subtle interplay between the effects due to the medium polarity and excitonic effects.¹⁷ A real understanding of the properties of these materials requires a detailed modeling of intermolecular interactions.

We describe the LB monolayer based on the same model recently proposed by two of the present authors for clusters of pp molecules.^{16,17} In particular, each chromophore is modeled in terms of the two-state Mulliken model discussed in the previous section, and intermolecular interactions only account for classical electrostatic forces (zero overlap approximation). The general Hamiltonian then reads:

$$\mathcal{H} = \sum_i (2z\hat{p}_i - \sqrt{2}t\hat{\sigma}_{x,i}) + \sum_{i,j>i} V_{ij}\hat{p}_i\hat{p}_j \quad (2)$$

with the sums running on all molecular sites. The first term describes the molecular two-state Hamiltonian: $\hat{p}_i = \sigma_{z,i} + 1/2$ measures the polarity of the i th chromophore, and $\sigma_{x/z,i}$ is the x/z -Pauli spin matrix for the i th site. The second term accounts for electrostatic intermolecular interactions, with V_{ij} measuring the interaction between two fully ionic ($|D^+A^- \rangle$) molecules at sites i and j . Since intermolecular distances are of the same order of magnitude as, or even smaller than, typical molecular lengths, the dipole approximation is inadequate, and we prefer to model the interactions by describing each $|D^+A^- \rangle$ as a segment of length l bearing a $\pm e$ charge at the D/A ends. For $C_{16}H_{33}Q$ -3CNQ we fix $l \approx 8\text{ \AA}$, as derived from the estimated value of the dipole moment μ_0 (see previous section). To model LB films we then consider a square lattice of molecules in the x,y plane, with intermolecular distances $r \sim 7\text{ \AA}$ to reproduce the experimentally determined area per molecule $\sim 50\text{ \AA}^2$.¹⁰ The molecular dipoles make a finite angle, ϕ , with the z -axis, and to relieve steric hindrance, we rotate the dipole in the x,y plane by an angle that we arbitrarily fix at 30° . The tilt angle ϕ is then the only adjustable parameter. For sure, the model adopted for the film is fairly crude, and the imposed geometry is somewhat arbitrary: our aim here is just to show that, based on the model parameters for $C_{16}H_{33}Q$ -3CNQ extracted from the analysis of solution spectra, we can construct a reasonable model for LB films. Moreover, and even more important, on the basis of this simplified picture we can discriminate between the different roles of environmental polarity and exciton motion in determining the spectroscopic behavior of the film.

The Hamiltonian in eq 2 describes only electronic degrees of freedom, but from the analysis of solution spectra in the previous section, we know that electron-vibration coupling must also be accounted for. Solving the complete electronic and vibrational problem on the lattice is challenging, but it is not really needed for the specific case. In fact, absorption spectra measured for the LB films are very narrow, suggesting that the exciton hopping in the lattice is faster than typical vibrational motion:^{35,36} the molecules have no time to relax their geometry upon photoexcitation, and the typical vibronic structure of

electronic transitions is lost. In other terms, the lack of vibronic structure in the absorption spectra of the LB film implies that the photoexcited state is largely delocalized so that the nuclear displacement associated with photoexcitation in the isolated (solvated) molecule is smeared out over many molecules, leading to vanishing spectroscopic effects of e-ph coupling.³⁷ So, to calculate reliable electronic spectra, we just need to solve the electronic Hamiltonian. However, care has to be taken, since the electron-vibration coupling enters in the definition of the gs molecular geometry: the relevant electronic Hamiltonian then must refer to molecules in the gs equilibrium geometry. This requirement is easily implemented, in fact Holstein coupling in the adiabatic approximation enters the electronic Hamiltonian by introducing a Q -dependent $z = z_0 - \sqrt{\epsilon_1/2\omega_1}Q_1$. The Hellmann–Feynman theorem gives a simple relation between the coupled coordinate Q_1 and the molecular polarity $Q_1 = (\sqrt{2\epsilon_1/\omega_1})\rho$.⁶ The electronic Hamiltonian then coincides with the original Mulliken Hamiltonian, but with the energy gap between the two basis states self-consistently dependent on the gs polarity: $z = z_0 - \epsilon_1\rho$.⁶

The solution of the problem then goes as follows: we diagonalize the Hamiltonian in eq 2 for a fixed lattice geometry and several z values. Exact diagonalization is performed on finite size (4×4) molecular clusters, the basis set being obtained from the direct product of the two basis states ($|DA\rangle$ and $|D^+A^-\rangle$) for each site.^{16,17} We impose periodic boundary conditions to minimize finite size effects and take advantage of translational symmetry. From the gs eigenstate we calculate $\rho(z)$, and using the ϵ_1 value in Table 1, we can finally evaluate $z_0 = z + \epsilon_1\rho$ and accept the result only if this number coincides within 0.001 with the reference $z_0 = -0.25$ eV value estimated from solution measurements (cf. Table 1). For the relevant z , the complete diagonalization of the Hamiltonian leads to the electronic spectrum.

The experimental spectra of LB films, with absorption peaking at 550–570 nm, are reproduced for $\phi \approx 77.5^\circ$, corresponding to Madelung energy $M \approx -0.957$ eV and $\rho \approx 0.97$. We emphasize that this estimate is based on the molecular parameters z_0 , $\sqrt{2}t$, and ϵ_1 reported in Table 1, as obtained from the analysis of solution spectra. As discussed in the previous section, these parameters actually refer to the solvated and not to a gas-phase molecule, since they account for the effects of the electronic polarization of the surrounding medium. Transferring these parameters to model LB films or other samples implies the tacit assumption that the fast electronic degrees of freedom of the surrounding have similar effects in the different phases. This fairly crude approximation can, however, be justified, based on the similarity of refractive indexes in organic matrices, either solutions or solid phases.

It is useful to compare the exact solution of the Hamiltonian in eq 2 with a mean-field (mf) solution. Within mf the cluster of interacting molecules is described as a collection of noninteracting molecules each one subject to the electrostatic field generated by the surrounding molecules.¹⁷ The mf Hamiltonian then coincides with the self-consistent two-state Mulliken Hamiltonian relevant to a solvated DA chromophore^{4,7} but with the Madelung energy, M , playing exactly the same role as $-\epsilon_{or}$. The experimental absorption at ~ 550 – 570 nm leads within mf to the following estimates: $\phi \approx 75.5^\circ$, $\rho \approx 0.96$, and $M \approx -0.663$ eV. The similarity between mf and exact estimates of ρ suggests that the excitonic and ultraexcitonic corrections to the energy of the allowed transition are small. Indeed, the excitonic correction to the absorption frequency is very small: $E_{exc} = 2M\rho(1 - \rho) \approx 0.06$ eV, and ultraexcitonic corrections

to the frequency turn out to be of the same order of magnitude. We can therefore conclude that the mf approximation leads to a reasonably accurate estimate of the absorption frequency of LB films of $C_{16}H_{33}Q$ -3CNQ. This means that the blue-shift of the absorption band from solution to LB films is essentially due to the increased polarity of the medium. The excitonic shift is minor in magnitude, and actually drives the absorption slightly to the red with respect to the mf result: in the LB film, in fact, intermolecular interactions are globally attractive ($M < 0$) so that J -type excitonic effects are observed. This is a very strong demonstration that common arguments must be considered with care, when applied to supramolecular architectures of polar and polarizable chromophores, where the effects of the medium polarity can be very large, and in some cases (as in the present one) largely dominate the observed shifts.

We notice that the estimated exciton shift, ~ 0.06 eV (500 cm^{-1}), is smaller than the vibrational frequency of the effective Holstein mode. This, however, does not contrast with the observation of narrow absorption bands in the LB film. In fact, the exciton shift goes with the Madelung energy, which in the specific case is a fairly small quantity, deriving from the cancellation of large positive and negative contributions. The exciton mobility instead increases with the *absolute* value of the interactions, and we estimate the effective excitonic bandwidth as ~ 0.5 eV, a few times larger than the vibrational frequency.

As we stressed above, the adopted model for the structure of the LB film is very simple: to calculate intermolecular interactions we approximate the molecular charge distribution as a dipole of finite length, an approximation that most probably overestimates electrostatic interactions. The lattice geometry, the length of the dipole, and the intermolecular distance are based on reasonable, but far from unique choices. Calculated spectra are a smooth function of the intermolecular distance and of the angle defining the rotation in the x – y plane, whereas they depend strongly on ϕ : this is the main reason to use ϕ as the adjustable parameter. The $\phi \approx 75^\circ$ – 77° value extracted from the fit is indeed fairly large, if compared with the experimental value $40 \div 45^\circ$.^{11,18} We observe, however, that the experimental estimate is based on the ratio between the film thickness and the estimated molecular length, so that is fairly uncertain by itself. Moreover, and more important, our estimate corresponds to an effective angle, which accounts for other phenomena (including disorder) that are not explicitly accounted for in the simple model. In addition, our exact results are based on a fairly small molecular cluster of 4×4 molecules. Extending the system size reduces the estimate of ϕ . To appreciate this point, we can compare with mf results, which, as discussed above, lead to a fairly reliable description of the excitation spectrum of LB films. Within mf, the absorption frequency of a 1000×1000 cluster coincides with the experimental value for $\phi \approx 68.5^\circ$.

5. Discussion and Conclusions

Understanding environmental effects on optical properties of pp chromophores is a first basic step toward the more general problem of environmental and supramolecular effects in molecular functional materials. In this paper we have presented a step-by-step analysis of environmental effects on optical spectra of $C_{16}H_{33}Q$ -3CNQ, an interesting dye that shows an impressive inverse solvatochromism and whose LB films behave as electrical rectifiers. Our approach starts with a thorough study of absorption and emission spectra in solution. The information gained at the molecular level is then transferred to the description

of LB films, leading to an internally consistent picture of the complex evolution of optical spectra of $C_{16}H_{33}Q-3CNQ$ with the local molecular environment. The analysis is based on a two-state description of the electronic structure of pp chromophores. This description, although simple, captures the relevant physics,^{6,7,21} and fully accounts for the molecular polarity and polarizability, the two properties that make environmental and supramolecular interactions particularly important and nontrivial.^{16,17}

The model proposed to describe solution spectra corresponds to a Mulliken model extended to account for Holstein coupling to molecular vibrations and to an effective solvation coordinate. This model has already been successfully applied to describe vibrational and optical spectra of pp chromophores with a neutral gs and hence normal solvatochromic (bathochromic) behavior.^{4,21–23} Here we use the same model for a zwitterionic dye, showing inverse solvatochromism (hypsochromism). The model nicely reproduces the most important spectral features, including frequencies, intensities, and band shapes, based on a few molecular parameters that are kept fixed in all solvents, and tuning a single parameter that accounts for the solvent polarity. Moreover, the complex evolution of absorption and emission band shapes with solvent polarity, and the nonspecularity of absorption and emission bands, are naturally obtained as a direct consequence of the polar and polarizable nature of D- π -A dyes. In this respect we emphasize that our approach gives the first rationalization of the distinctively different effects of the solvent polarity on absorption band shapes of normal and inverse solvatochromic dyes. At the same time the proposed picture describes narrower emission than absorption bands for both normal and inverse solvatochromic dyes, with particularly impressive effects for zwitterionic dyes dissolved in polar solvents.

The two-state model adopted for the electronic structure of solvated pp chromophores lends itself to describe the corresponding supramolecular architectures. Classical electrostatic interactions are the dominant intermolecular interactions in molecular materials made up of polar chromophores. We have recently demonstrated that in clusters of pp chromophores, as described within the Mulliken approximation, electrostatic interactions are responsible for the appearance of notable cooperative and collective phenomena that largely affect the material properties.^{16,17} In this paper we adopt the same Hamiltonian to describe the absorption spectra of LB films of $C_{16}H_{33}Q-3CNQ$. The present one is the first application of the model to a real experimental aggregate of pp chromophores, and its success affords good evidence for the reliability of the proposed approach.

We have shown that the standard excitonic description of optical spectra of molecular materials can be misleading if applied to materials made up of pp chromophores. The observed blue-shift of the absorption band from solution to the LB film in fact is not due to H-exciton effects, i.e., to collective effects related to the presence of repulsive intermolecular interactions,³⁸ but is rather dominated by mf effects, i.e., by the average polarity of the surrounding medium. In the film intermolecular interactions are indeed attractive, and excitonic effects actually shift the absorption slightly to the red with respect to the mf frequency. We underline that the mf correction to the excitation energy can be assimilated to the so-called gas to crystal shift (the *D*-term correction) of the excitonic model.^{38,39} However, in the exciton model any mixing between the ground and the excited states is disregarded so that only energies and not wave functions can be affected by the environment:¹⁷ the variation

of the molecular polarity with the environment and its spectral consequences are beyond the excitonic model. The standard exciton model, originally developed for materials based on nonpolar and hardly polarizable molecules,³⁹ fully neglects the molecular polarizability: its extension to materials based on pp molecules requires the proper definition of a mf gs for polarizable molecular units.¹⁷

An interesting model for materials made up of nonpolar but polarizable molecules has been recently proposed,⁴⁰ where classical electrostatic intermolecular interactions are treated in mf approximation. The model, based on a quantum-chemical description of the molecular units, nicely demonstrates the importance of supramolecular electrostatic interactions in the definition of the material properties. *Cooperative* effects are shown to be important in establishing the value of the dielectric constant⁴⁰ and other gs properties. Apart from a narrow region near discontinuous crossovers, the cooperative effects are well accounted for in a mf approximation.^{17,41} *Collective* (excitonic) effects, on the other hand, are generally important for spectral properties, and go beyond the mf approximation. In the specific case of $C_{16}H_{33}Q-3CNQ$ LB films, cooperative effects dominate over collective effects in determining the absorption frequency, so that the mf approximation holds. Collective effects, however, show up in the narrow shape of the absorption spectrum of the LB film.

The supramolecular geometry, adopted to describe LB monolayers of $C_{16}H_{33}Q-3CNQ$, is plausible, but somewhat arbitrary. Moreover, our exact results, obtained for a square lattice of 16 molecules, are affected by finite-size effects. Despite these obvious limitations, our analysis demonstrates that it is possible to understand the basic physics underlying the complex spectroscopic behavior of $C_{16}H_{33}Q-3CNQ$ based on a fairly simple model. In particular, molecular parameters, obtained from solution spectra, can be adopted to reproduce absorption spectra of the same molecule in different environments, provided intermolecular interactions are properly accounted for. As is often the case when modeling complex phenomena, the equilibrium between accuracy and simplicity is delicate. Despite its many limitations, the proposed approach offers the possibility to predict the properties of molecular materials based on the spectroscopic properties of the solvated molecules. For sure further theoretical and experimental work is needed to gain confidence on the proposed approach, yet the first example of *bottom-up modeling* presented here nicely parallels the bottom-up strategy of synthetic chemists, and opens the way to extend the structure-properties relationships from the molecular to the supramolecular level, as required to guide the design of molecular materials with optimized functional behavior.

Acknowledgment. The work in Parma has been supported by the Consorzio Interuniversitario per la Scienza e Tecnologia dei Materiali (INSTM) through the PRISMA 2002 project, and by the Italian Ministry of Instruction, University and Research (MIUR) through the FIRB 2003 project. The work at the University of Alabama was supported by the United States National Science Foundation (grants DMR-00-9215, DMR-00-99674, and DMR-01-20967).

References and Notes

- (1) Kanis, D. R.; Ratner, M. A.; Marks, T. J. *Chem. Rev.* **1994**, *94*, 195.
- (2) Marder, S. R.; Kippelen, B.; Jen, A. K.-Y.; Peyghambarian, N. *Nature* **1997**, *388*, 845.
- (3) Brédas, J. L.; Cornil, K.; Meyers, F.; Beljonne, D. In *Handbook of Conducting Polymers*, 2nd ed.; Skotheim, T. A., Elsenbaumer, R. L., Reynolds, J. R., Eds.; Marcel Dekker: New York, 1998; p 1.

- (4) Boldrini, B.; Cavalli, E.; Painelli, A.; Terenziani, F. *J. Phys. Chem. A* **2002**, *106*, 6286.
- (5) Oudar, J. L.; Chemla, D. S. *J. Chem. Phys.* **1977**, *66*, 2664.
- (6) Painelli, A. *Chem. Phys. Lett.* **1998**, *285*, 352.
- (7) Painelli, A. *Chem. Phys.* **1999**, *245*, 183.
- (8) Reichardt, C. *Chem. Rev.* **1994**, *94*, 2319.
- (9) Ashwell, G. J. In *Organic Materials for Nonlinear Optics*; Ashwell, G. J., Bloor, D., Eds.; Royal Society of Chemistry: Cambridge, UK, 1993; pp 31–39.
- (10) Metzger, R. M.; Chen, B.; Höpfner, U.; Lakshmikantham, M. V.; Vuillaume, D.; Kawai, T.; Wu, X.; Tachibana, H.; Hughes, T. V.; Sakurai, H.; Baldwin, J. W.; Hosch, C.; Cava, M. P.; Brehmer, L.; Ashwell, G. J. *J. Am. Chem. Soc.* **1997**, *119*, 10455.
- (11) Metzger, R. M. *Chem. Rev.* **2003**, *103*, 3802.
- (12) Myers Kelley, A. B. *J. Phys. Chem. A* **1999**, *103*, 6891.
- (13) Painelli, A.; Del Freo, L.; Terenziani, F. In *Molecular Low Dimensional Materials for Advanced Applications*; Graja, A., Agranovich, V. M., Kajzar F., Eds.; Kluwer Academic Publisher: Dordrecht, The Netherlands, 2002; p 113.
- (14) Soos, Z. G.; Painelli, A.; Girlando, A.; Mukhopadhyay, D. In *Handbook of Conducting Polymers*, 2nd ed.; Skotheim, T. A., Elsenbaumer, R. L., Reynolds, J. R., Eds.; Marcel Dekker: New York, 1998; p 168.
- (15) Krugler, J. L.; Montgomery, C. G.; McConnell, H. M. *J. Chem. Phys.* **1964**, *41*, 2421.
- (16) Painelli, A.; Terenziani, F. *J. Am. Chem. Soc.* **2003**, *125*, 5624.
- (17) Terenziani, F.; Painelli, A. *Phys. Rev. B* **2003**, *68*, 165405.
- (18) Baldwin, J. W.; Chen, B.; Street, S. C.; Kononov, V. K.; Sakurai, H.; Hughes, T. V.; Simpson, C. S.; Lakshmikantham, M. V.; Cava, M. P.; Kispert, L. D.; Metzger, R. M. *J. Phys. Chem. B* **1999**, *103*, 4269.
- (19) Bell, N. A.; Broughton, R. A.; Brooks, J. S.; Jones, T. A.; Thorpe, S. C.; Ashwell, G. J. *J. Chem. Soc., Chem. Commun.* **1990**, 325.
- (20) Ashwell, G. J.; Jefferies, G.; Dawney, E. J. C.; Kuczynski, A. P.; Lynch, D. E.; Gongda, Y.; Bucknall, D. G. *J. Mater. Chem.* **1995**, *5*, 975.
- (21) Painelli, A.; Terenziani, F. *Chem. Phys. Lett.* **1999**, *312*, 211.
- (22) Painelli, A.; Terenziani, F. *J. Phys. Chem. A* **2000**, *104*, 11041.
- (23) Terenziani, F.; Painelli, A.; Comoretto, D. *J. Phys. Chem. A* **2000**, *104*, 11049.
- (24) Terenziani, F.; Painelli, A. In *Organic Nanostructures: Science and Applications*; Agranovich, V. M., La Rocca, G. C., Eds.; Proc. Int. School Phys. “E. Fermi” Course CXLIX, IOS Press: Amsterdam, The Netherlands, 2002; p 569.
- (25) Terenziani, F.; Painelli, A. *Chem. Phys.* **2003**, *295*, 35.
- (26) Mulliken, R. S. *J. Am. Chem. Soc.* **1952**, *74*, 811.
- (27) Lu, D.; Chen, G.; Perry, J. W.; Goddard, W. A. *J. Am. Chem. Soc.* **1994**, *116*, 10679.
- (28) Barzoukas, M.; Fort, A.; Blanchard-Desce, M. *Chem. Phys. Lett.* **1996**, *257*, 531.
- (29) Kim, H.-S.; Cho, M.; Jeon, S.-J. *J. Chem. Phys.* **1997**, *107*, 1936.
- (30) Liptay, W. *Angew. Chem.* **1969**, *8*, 177. Di Bella, S.; Marks, T. J.; Ratner, M. A. *J. Am. Chem. Soc.* **1994**, *116*, 4440.
- (31) Painelli, A.; Terenziani, F. *Synth. Met.* **2001**, *116*, 135.
- (32) Metzger, R. M. *J. Mater. Chem.*, **2000**, *10*, 55.
- (33) Bozio, R.; Zanon, I.; Girlando, A.; Pecile, C. *J. Chem. Soc., Faraday Trans. 2* **1978**, *74*, 235.
- (34) Xu, T.; Morris, T. A.; Szulcowski, G. J.; Amaresh, R. R.; Gao, Y.; Street, S. C.; Kispert, L. D.; Metzger, R. M.; Terenziani, F. *J. Phys. Chem. B* **2002**, *106*, 10374.
- (35) Fulton, R. L.; Gouterman, M. *J. Chem. Phys.* **1964**, *41*, 2280.
- (36) Myers Kelley, A. *J. Chem. Phys.* **2003**, *119*, 3320.
- (37) Feinberg, D.; Ciuchi, S.; de Pasquale, F. *Int. J. Mod. Phys. B* **1990**, *4*, 1317.
- (38) Knoester, J. In *Organic Nanostructures: Science and Applications*; Agranovich, V. M., La Rocca, G. C., Eds.; Proc. Int. School Phys. “E. Fermi” Course CXLIX, IOS Press: Amsterdam, The Netherlands, 2002; p 149 and references therein.
- (39) Agranovich V. M.; Galanin, M. D. *Electronic Excitation Energy Transfer in Condensed Matter*, North-Holland, Amsterdam, 1982.
- (40) Tsiper, E. V.; Soos, Z. G. *Phys. Rev. B* **2003**, *68*, 85301.
- (41) Painelli, A.; Terenziani, F. *Synth. Met.* **2001**, *116*, 135.